



## Research Article

# Synthesis of silica xerogel@Mg-Al layered double hydroxide composite for CO<sub>2</sub> capture

Dicle EREN<sup>1</sup>, Muge SARI YILMAZ<sup>1,\*</sup>

<sup>1</sup>Faculty of Chemical and Metallurgical Engineering, Yildiz Technical University, İstanbul, Türkiye

## ARTICLE INFO

### Article history

Received: 07 November 2022

Revised: 04 January 2023

Accepted: 08 February 2023

### Keywords:

CO<sub>2</sub> Capture; Kinetics; Layered Double Hydroxide; Xerogel

## ABSTRACT

Today, the increase in the level of carbon dioxide (CO<sub>2</sub>) gas in the atmosphere has started to cause concern. Therefore, an appropriate and rapid decrease in CO<sub>2</sub> gas emission levels has become a significant challenge. Capturing CO<sub>2</sub> on a solid surface is proposed due to its ease of application, relatively low energy requirements, and applicability in various processes. This study investigated the preparation of Xerogel@MgAl LDH (X@MAL) composite for CO<sub>2</sub> capture. Firstly, silica-based xerogel was synthesized by the acid and base-catalyzed two-step sol-gel method. Then, the X@MAL composite was prepared by the co-precipitation method. Based on the CO<sub>2</sub> capture analysis, the maximum CO<sub>2</sub> capture capacity of the composite at 25 °C, 75 °C, and 100 °C was 1.90 mmol.g<sup>-1</sup>, 0.70 mmol.g<sup>-1</sup>, and 0.40 mmol.g<sup>-1</sup>, respectively. The kinetic analysis results show that the CO<sub>2</sub> capture of X@MAL can be well-defined by Avrami kinetic model.

**Cite this article as:** Eren D, Sarı Yılmaz M. Synthesis of silica xerogel@Mg-Al layered double hydroxide composite for CO<sub>2</sub> capture. Sigma J Eng Nat Sci 2024;42(4):1101–1107.

## INTRODUCTION

Emissions of CO<sub>2</sub> into the atmosphere are increasing significantly due to the energy industry, transportation sector, and human activities [1]. The excessive increase in the concentration of greenhouse gases, especially CO<sub>2</sub>, is due to the burning of fossil fuels, which causes global warming and other environmental effects [2]. It is extremely important to develop technologies that reduce greenhouse gas emissions [3].

Therefore, the most promising method to mitigate the impact of CO<sub>2</sub> on global climate is CO<sub>2</sub> capture from fossil fuels consumed by power plants. The process economies of such technologies are often not cheap enough to offset the

hold costs. Thus, it is highly desirable to develop alternatives that are more energy efficient than conventional separation technologies.

Among these techniques, adsorption is one of the most promising approaches as it can reduce the costs associated with the hold step. In general, high CO<sub>2</sub> capture capacity, high selectivity, low material cost, and stable adsorption capacity after several cycles are the main characteristics of CO<sub>2</sub> adsorbents [3].

Recently, scientists have made dramatic efforts to produce suitable adsorbents capable of meeting the requirements of CO<sub>2</sub> emission sources. Many of the scientific community have worked on the development of various types of porous solid adsorbents based on activated carbon

### \*Corresponding author.

\*E-mail address: [mugesari@yildiz.edu.tr](mailto:mugesari@yildiz.edu.tr)

This paper was recommended for publication in revised form by Editor in-Chief Ahmet Selim Dalkilic



[4,5], mesoporous silica materials [6,7], zeolites [8], metal-organic frameworks (MOFs) [9], mesocellular foams [10], and layered double hydroxides (LDHs) [11].

LDHs are inorganic materials that are members of the family of two-dimensional clay minerals with multiple metal cations in their inner layers and anions in their interlayers. The structure of LDHs consist of brushite  $[\text{Mg}(\text{OH})_2]^{+}$  like positively charged metal hydroxide layers and anions and water molecules that exist as charge balancers between the layers. The potential use of LDHs in high-temperature carbon capture and storage applications is promising [12]. LDHs require less energy for regeneration in  $\text{CO}_2$  adsorption and show better stability than some solid adsorbents [13]. They also show rapid adsorption-desorption kinetics, especially in the presence of water. This has made LDHs interesting in pre-combustion  $\text{CO}_2$  capture applications [14,15].

Xerogels are used as supporting materials in the preparation of various composites due to their unique properties [16,17]. By uniting LDHs with xerogel, which is found in different forms such as a monolith, powder, fiber, or film, composite materials with superior properties are created.

Xerogels are generally prepared by the sol-gel method under atmospheric pressure. Some properties such as the pore of xerogels can scale, high surface area, low intensity, thermal conductivity, dielectric constant, high optical permeability in visible light, and sound insulation of this material make it unique for several scientific and technological applications [18]. The brittleness, moisture-holding, and instability of silica xerogels in long-term applications can limit the use of these materials. These disadvantages can be eliminated with surface modification, heat treatment, or preparation of composite materials by adding various fillers [19].

To the author's knowledge, only one study has been found in the literature on the combination of xerogel with MgAl LDH. Okada et al. prepared the MgAl LDH and aluminosilicate xerogel composites for  $\text{CO}_2$  and  $\text{NH}_3$  gas adsorption [20]. The composition of xerogel and the synthesis procedure of the composite differs from our study.

In this study, X@MAL composite was synthesized for the first time for  $\text{CO}_2$  capture application. Firstly, silica-based xerogel was synthesized by the acid and base-catalyzed two-step sol-gel method. Then, the X@MAL composite was prepared by the co-precipitation method by using the synthesized xerogel. The obtained material was characterized by X-ray diffraction (XRD) and Fourier transform infrared (FTIR) analysis. The  $\text{CO}_2$  capture capacity of the composite was carried out using by gravimetric method at different adsorption temperatures.

## EXPERIMENTAL PROCEDURES

### Materials and Characterization

The materials used in the xerogel synthesis were supplied by Sigma-Aldrich. For the synthesis of X@MAL composite

magnesium nitrate hexahydrate ( $\text{Mg}(\text{NO}_3)_2 \cdot 6\text{H}_2\text{O}$ , Merck) aluminum nitrate nonahydrate ( $\text{Al}(\text{NO}_3)_3 \cdot 9\text{H}_2\text{O}$ , Merck), sodium hydroxide (NaOH, Merck) sodium carbonate ( $\text{Na}_2\text{CO}_3$ , Merck) were used.

The characterization analysis of the composite was carried out using a PANalytical X'Pert-Pro XRD diffractometer and Perkin-Elmer Spectrum One FT-IR spectrophotometer. The XRD measurements of xerogel and X@MAL composite were taken in the  $2\theta$  range from  $5^\circ$  to  $100^\circ$ .

Infrared spectra were collected using the KBr pellet technique in absorbance mode within the range from  $4000$  to  $450 \text{ cm}^{-1}$ .

The  $\text{CO}_2$  capture analysis of the composite was studied using Perkin Elmer Pyris Diamond thermogravimetric equipment. In the capture analysis, pure  $\text{CO}_2$  (>99.99%) gas was used.

Briefly, approximately 10 mg of sample was put in an alumina crucible, and then, it was heated to  $105^\circ\text{C}$  under a nitrogen atmosphere to remove its moisture. Afterward, the ambient temperature was reduced to a specific temperature at a cooling rate of  $10^\circ\text{C} \cdot \text{min}^{-1}$ . For the capture analysis, the gas was changed to  $\text{CO}_2$  at a flow rate of 100 ml per minute for 90 minutes. The weight increase of the sample was used to determine the sample's  $\text{CO}_2$  capture capacity.

### Synthesis of X@MAL Composite

To synthesize the X@MAL composite, the xerogel was first synthesized using our previous synthesis procedure available in the literature [21].

For the synthesis of the X@MAL composite, two different solutions were prepared. Initially, 0.1 g xerogel was dissolved in distilled water under ultrasonic irradiation. Then,  $\text{Na}_2\text{CO}_3$  is added to the xerogel solution and it continued the mixing for a while. The obtained solution was named the first solution and its pH of it was adjusted to 10. In order to prepare the second solution, 0.25 g  $\text{Mg}(\text{NO}_3)_2 \cdot 6\text{H}_2\text{O}$  and 0.18 g  $\text{Al}(\text{NO}_3)_3 \cdot 9\text{H}_2\text{O}$  were dissolved in the distilled water under ultrasonic irradiation. The obtained second solution is slowly added to the first solution under stirring at room temperature. The resultant solution was continued to stir for 1 hour at room temperature. At the end of the time, the precipitation was collected by centrifugation, and then, it is washed with distilled water and ethanol separately. Finally, it was centrifuged again and dried under a vacuum.

## RESULTS AND DISCUSSION

### Characterization of Adsorbent

Figure 1 demonstrates the XRD pattern of xerogel and X@MAL composite. The XRD analysis of xerogel showed one broad diffraction peak observed between  $20$ - $30^\circ$  indicating its amorphous structure [22]. In the XRD analysis of the X@MAL composite, the characteristic amorphous peak of xerogel and newly formed (003), (009), (015), and (110) diffraction peaks related to the LDH phase were seen,

indicating that the layered Mg-Al LDH was formed in the xerogel structure. The characteristic (006) peak of Mg-Al LDH overlapped with the broad peak of xerogel, therefore the (006) peak of Mg-Al LDH was not observed in the patterns of X@MAL.

The FT-IR spectrum of xerogel and X@MAL composite were given in Figure 2. In the FT-IR spectrum of xerogel, the characteristic peak at  $1087\text{ cm}^{-1}$  corresponded to the asymmetric stretching of Si-O-Si groups [23]. The peaks at  $3448\text{ cm}^{-1}$  and  $1636\text{ cm}^{-1}$  were related to physically adsorbed water or structural -OH groups and adsorbed water molecules, respectively [24]. The Si-OH stretching vibration was observed at  $946\text{ cm}^{-1}$  [25]. The peaks at  $797\text{ cm}^{-1}$  and  $467\text{ cm}^{-1}$  were attributed Si-O-Si symmetric stretching vibrations and bending mode, respectively [26]. Compared with xerogel, the new peaks at around  $1498$  and  $1385\text{ cm}^{-1}$  were observed in the composite, which can be attributed to the vibrations of carbonate species originating from the LDH structure. In addition, differences were observed in the  $1000\text{-}450\text{ cm}^{-1}$  region due to the stretching of the Al-O and Mg-O metal-oxygen bonds [27–29].

### CO<sub>2</sub> Capture Measurement

The amounts of captured CO<sub>2</sub> at different temperatures ( $25^\circ\text{C}$ ,  $75^\circ\text{C}$ , and  $100^\circ\text{C}$ ) were given in Figure 3. The CO<sub>2</sub> capture capacity of the X@MAL composite decreases with increasing temperature, which is characteristic of physisorption. The CO<sub>2</sub> capture capacity at  $75^\circ\text{C}$  and  $100^\circ\text{C}$  remained constant after 35 minutes, while its capacity at  $25^\circ\text{C}$  remained stable after 80 minutes. The adsorption capacities of the X@MAL composite at different temperatures followed by following trend:  $1.90\text{ mmol.g}^{-1}$  ( $25^\circ\text{C}$ ) >  $0.70\text{ mmol.g}^{-1}$  ( $75^\circ\text{C}$ )

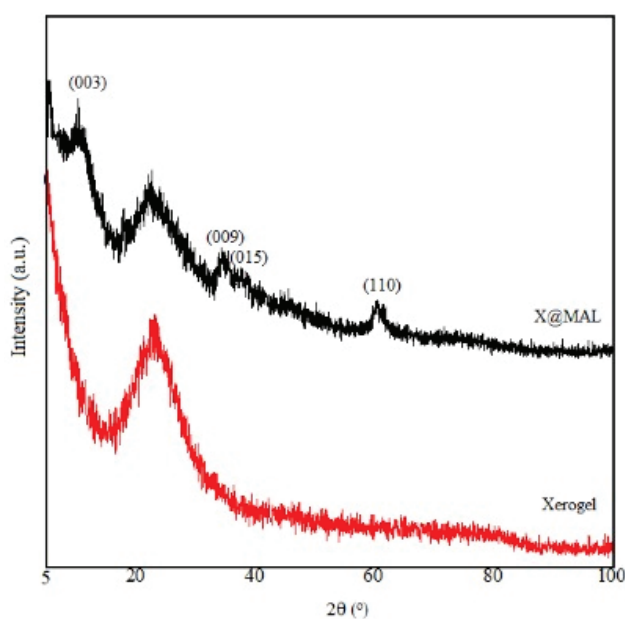


**Figure 1.** The XRD patterns for silica based xerogel and the X@MAL

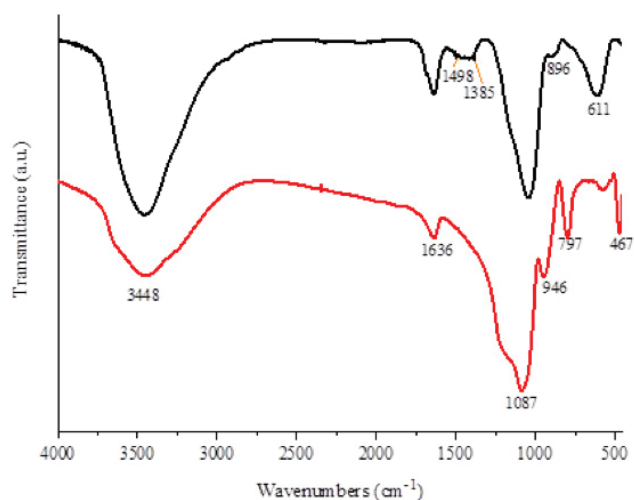


**Figure 2.** FTIR spectrum of composite (black line) and xerogel (red line).

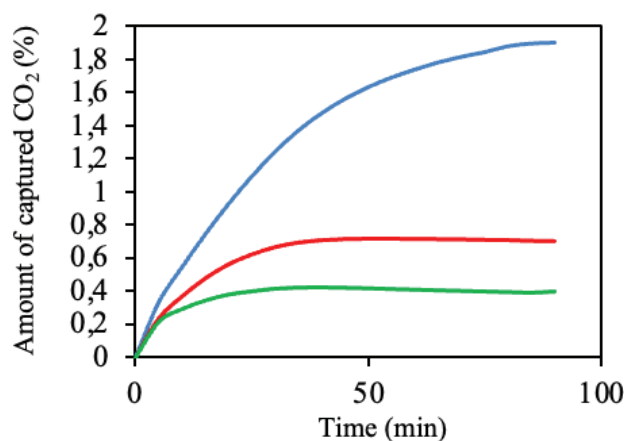


**Figure 3.** The CO<sub>2</sub> capture capacities of X@MAL composite at different temperatures (Blue line:  $25^\circ\text{C}$ , green line:  $75^\circ\text{C}$ , and red line:  $100^\circ\text{C}$ ).

>  $0.40\text{ mmol.g}^{-1}$  ( $100^\circ\text{C}$ ). At  $25^\circ\text{C}$ , the X@MAL exhibited approximately 5 times more capacity than the adsorption capacity at  $100^\circ\text{C}$ . Accordingly, it was observed that the CO<sub>2</sub> adsorption capacity of X@MAL decreased with the increase in temperature. This indicates that the adsorption of CO<sub>2</sub> into the composite is an exothermic process.

### Kinetic Analysis

To determine the mechanism of CO<sub>2</sub> adsorption of X@MAL composite, several of the most common kinetic models from the pseudo-first-order (FO), the pseudo-second-order (SO), and the Avrami (Av) model were selected. By using the CO<sub>2</sub> adsorption results at different temperatures, the compatibility of these models with the experimental values will be tested.

FO model was proposed by Lagergren and assumes that the rate of adsorption is proportional to the number of free active sites on the accessible adsorbent surface [30]. This equation can be given by:

$$q_t = q_e [1 - \exp(-k_f t)] \tag{1}$$

where  $q_t$  (mg/g) and  $q_e$  (mg/g) are the amounts of adsorbed  $\text{CO}_2$  at time  $t$  (min) and equilibrium.  $k_f$  ( $\text{min}^{-1}$ ) is the FO rate constant.

SO model was proposed by Ho et al. [31]. The adsorption rate with respect to SO is directly proportional to the square of the number of free active sites on the adsorbent and the kinetic model is expressed by the equation given below.

$$q_t = \frac{q_e^2 k_s t}{1 + q_e k_s t} \tag{2}$$

where  $k_s$  (g/(mg.min)) is the SO rate constant.

The Avrami method is a first-order fractional kinetics for particle nucleation and has recently been used to describe  $\text{CO}_2$  capture on solid adsorbents [32,33]. This model was described using the following equation:

$$q_t = q_e [1 - \exp \exp (-(k_a t)^{n_a})] \tag{3}$$

Where  $k_a$  and  $n_a$  are the rate constant and kinetic order of Av, respectively.

The error was determined using the following equation to determine the accuracy of the kinetic model:

$$\text{Error}(\%) = \sqrt{\frac{\sum_{i=1}^p \left[ \frac{q_{e(\text{exp})} - q_{e(\text{model})}}{q_{e(\text{exp})}} \right]^2}{p - 1}} \times 100\% \tag{4}$$

where  $q_{e(\text{exp})}$  and  $q_{e(\text{model})}$  are the value of adsorption capacity experimentally and obtained from the fitted model, respectively and  $p$  is the number of total experimental data.

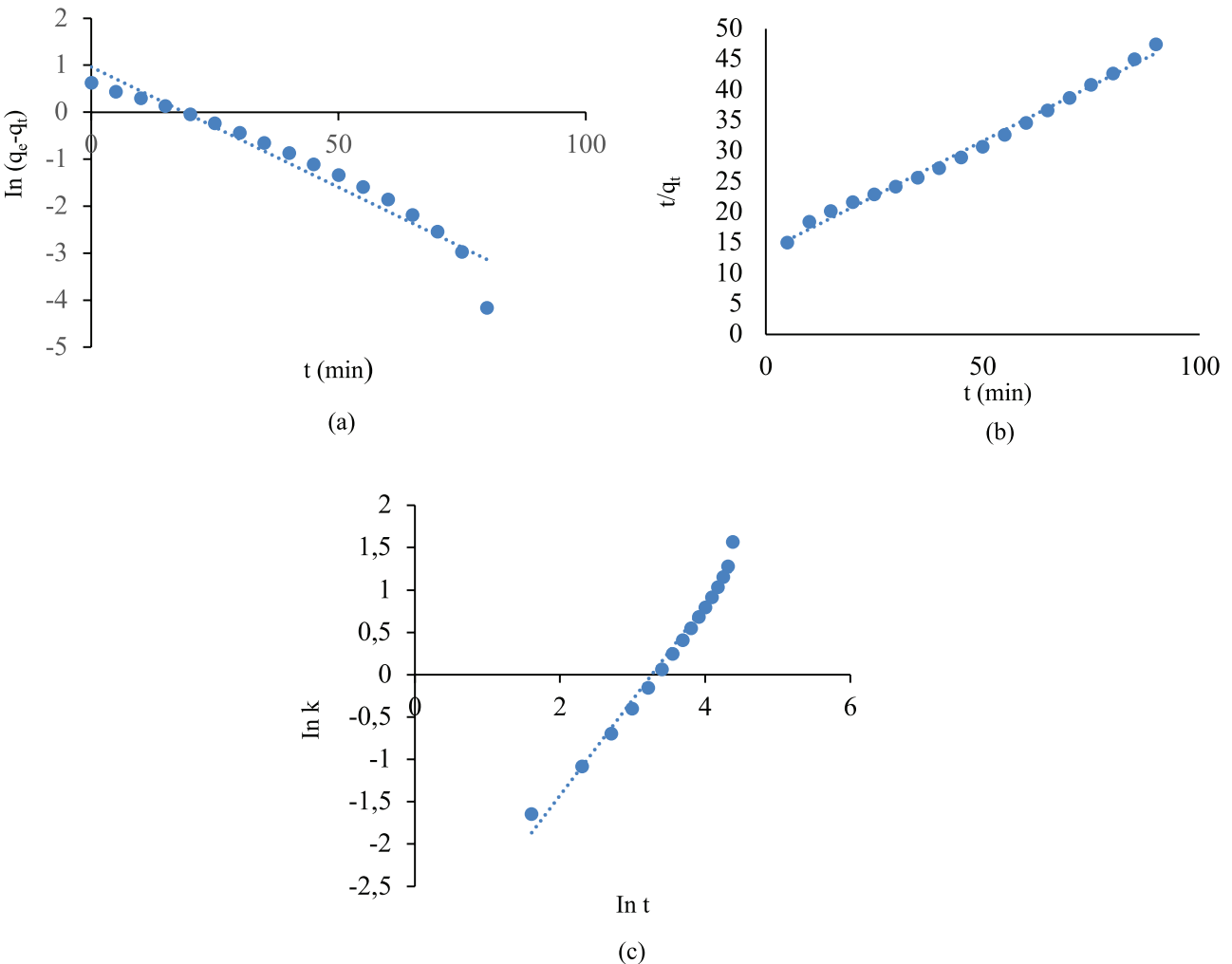
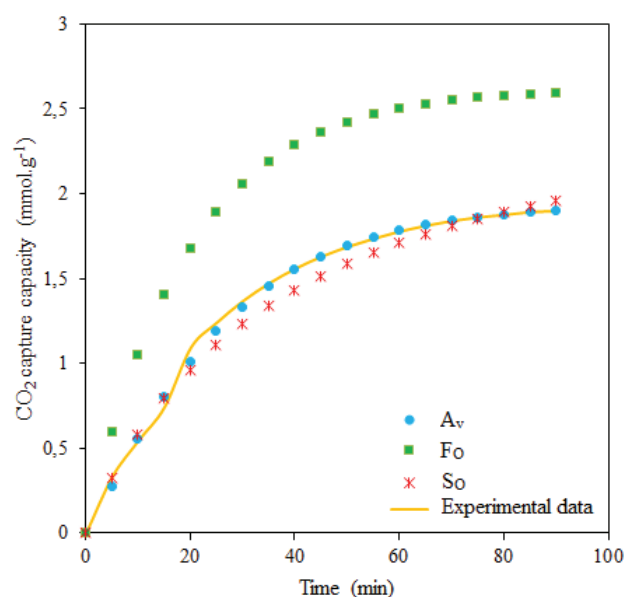


Figure 4. The kinetic model curves of  $\text{CO}_2$  capture on X@MAL at 25°C (a) FO, (b) SO, and (c) Av.

All kinetic models were fitted to explain the capture of CO<sub>2</sub> on X@MAL at 25°C (Figure 4). The calculated kinetic parameters of the fitted models are demonstrated in Table 1. It is seen that the SO provides the best fit among the three kinetic models as per the correlation coefficient (R<sup>2</sup>) values for X@MAL. However, it was found that the Av kinetic model presented a lower error value than the error values calculated from the FO and SO. In addition, when the fitted data shown in Figure 5 are examined, it is seen that the fitted data from the Av model are very close to the experimental data. Thus, the Av model is applied to predict the CO<sub>2</sub> capture process

**Table 1.** The kinetic parameters for CO<sub>2</sub> capture on X@MAL composite at 25°C

Kinetic Model	Parameter	Value
F <sub>O</sub>	q <sub>e, exp</sub> (mmol.g <sup>-1</sup> )	1.890
	k <sub>f</sub>	0.051
	R <sup>2</sup>	0.941
	Error (%)	9.712
S <sub>O</sub>	q <sub>e</sub> (mmol.g <sup>-1</sup> )	2.624
	k <sub>s</sub>	0.010
	R <sup>2</sup>	0.994
	Error (%)	11.363
A <sub>v</sub>	q <sub>e</sub> (mmol.g <sup>-1</sup> )	1.934
	k <sub>a</sub>	0.038
	n <sub>a</sub>	1.128
	R <sup>2</sup>	0.983
	Error (%)	0.600



**Figure 5.** Corresponding fit of X@MAL applying three kinetic models.

**Table 2.** Comparison of the CO<sub>2</sub> adsorption capacity of various composites

Adsorbent	Capacity (mmol.g <sup>-1</sup> )	References
<i>Silica xerogel-based</i>		
MMS-6	1.90	[3]
PEI functionalized xerogel	1.94	[34]
Polyurethane/ silica xerogels	1.10	[35]
<i>MgAl LDH-based</i>		
MgAl LDH	0.9	[36]
POM/MgAl LDH	0.74	[37]
GO/MgAl LDH	0.54	[38]
X@MAL	1.90	In this study

of X@MAL. The kinetic order of Av (n<sub>a</sub>) is found as 1.128 indicating the multiple kinetic order of the CO<sub>2</sub> capture.

#### Comparison with Other Adsorbents

A comparison of the CO<sub>2</sub> uptake capacity of silica xerogel and MgAl LDH-based adsorbents found in the literature are listed in Table 2. Compared with the silica xerogel-based adsorbents, X@MAL showed either close or better adsorption capacity. The CO<sub>2</sub> adsorption performance of X@MAL is superior to MgAl LDH-based adsorbents. Overall, it is seen that the X@MAL composite has a good enough capacity to compete with the adsorbents in the literature.

#### CONCLUSION

In this study, the X@MAL composite was prepared by the co-precipitation method. The XRD and FTIR characterization results showed that the composite was synthesized successfully. The CO<sub>2</sub> capture experiments at different temperatures indicated that the maximum capture capacity of the composite was 1.90 mmol.g<sup>-1</sup> at 25°C. Adsorption kinetics demonstrated that the Av model had a better fitting effect and was more suitable for describing the CO<sub>2</sub> capture process.

#### ACKNOWLEDGMENT

This work was supported by Yildiz Technical University Scientific Research Projects Coordination Unit. Project Number: FLY-2022-4884.

#### AUTHORSHIP CONTRIBUTIONS

Authors equally contributed to this work.

#### DATA AVAILABILITY STATEMENT

The authors confirm that the data that supports the findings of this study are available within the article. Raw

data that support the finding of this study are available from the corresponding author, upon reasonable request.

## CONFLICT OF INTEREST

The author declared no potential conflicts of interest with respect to the research, authorship, and/or publication of this article.

## ETHICS

There are no ethical issues with the publication of this manuscript.

## REFERENCES

- [1] Loganathan S, Tikmani M, Edubilli S, Mishra A, Ghoshal AK. CO<sub>2</sub> adsorption kinetics on mesoporous silica under wide range of pressure and temperature. *Chem Eng J* 2014;256:1–8. [\[CrossRef\]](#)
- [2] Aquino AS, Vieira MO, Ferreira ASD, Cabrita EJ, Einloft S, de Souza MO. Hybrid ionic liquid-silica xerogels applied in CO<sub>2</sub> capture. *Appl Sci* 2019;9:2614. [\[CrossRef\]](#)
- [3] Witoon T, Tatan N, Rattanavichian P, Chareonpanich M. Preparation of silica xerogel with high silanol content from sodium silicate and its application as CO<sub>2</sub> adsorbent. *Ceram Int* 2011;37:2297–2303. [\[CrossRef\]](#)
- [4] Serafin J, Sreńscek-Nazzal J, Kamińska A, Paszkiewicz O, Michalkiewicz B. Management of surgical mask waste to activated carbons for CO<sub>2</sub> capture. *J CO<sub>2</sub> Util* 2022;59:101970. [\[CrossRef\]](#)
- [5] Ismail IS, Rashidi NA, Yusup S. Production and characterization of bamboo-based activated carbon through single-step H<sub>3</sub>PO<sub>4</sub> activation for CO<sub>2</sub> capture. *Environ Sci Pollut Res Int* 2022;29:12434–12440. [\[CrossRef\]](#)
- [6] Sari Yilmaz M. The CO<sub>2</sub> adsorption performance of aminosilane-modified mesoporous silicas. *J Therm Anal Calorim* 2021;146:2241–2251. [\[CrossRef\]](#)
- [7] Sari Yilmaz M, Karakas SB. Low-cost synthesis of organic-inorganic hybrid MSU-3 from gold mine waste for CO<sub>2</sub> adsorption. *Water Air Soil Pollut* 2018;229:326. [\[CrossRef\]](#)
- [8] Choi HJ, Hong SB. Effect of framework Si/Al ratio on the mechanism of CO<sub>2</sub> adsorption on the small-pore zeolite gismondine. *Chem Eng J* 2022;433:133800. [\[CrossRef\]](#)
- [9] Lei L, Cheng Y, Chen C, Kosari M, Jiang Z, He C. Taming structure and modulating carbon dioxide (CO<sub>2</sub>) adsorption isosteric heat of nickel-based metal organic framework (MOF-74(Ni)) for remarkable CO<sub>2</sub> capture. *J Colloid Interface Sci* 2022;612:132–145. [\[CrossRef\]](#)
- [10] Bai F, Liu X, Sani S, Liu Y, Guo W, Sun C. Amine functionalized mesocellular silica foam as highly efficient sorbents for CO<sub>2</sub> capture. *Sep Purif Technol*. 2022;299:121539. [\[CrossRef\]](#)
- [11] Sari Yilmaz M. Synthesis of novel amine modified hollow mesoporous silica@Mg-Al layered double hydroxide composite and its application in CO<sub>2</sub> adsorption. *Microporous Mesoporous Mater* 2017;245:109–117. [\[CrossRef\]](#)
- [12] Garcia-Gallastegui A, Iruretagoyena D, Gouvea V, Mokhtar M, Asiri AM, Basahel SN, et al. Graphene oxide as support for layered double hydroxides: Enhancing the CO<sub>2</sub> adsorption capacity. *Chem Mater* 2012;24:4531–4539. [\[CrossRef\]](#)
- [13] Choi S, Drese JH, Jones CW. Adsorbent materials for carbon dioxide capture from large anthropogenic point sources. *ChemSusChem* 2009;2:796–854. [\[CrossRef\]](#)
- [14] Ding Y, Alpay E. Equilibria and kinetics of CO<sub>2</sub> adsorption on hydrotalcite adsorbent. *Chem Eng Sci* 2000;55:3461–3474. [\[CrossRef\]](#)
- [15] Van Selow ER, Cobden PD, Verbraeken PA, Hufton JR, Van Den Brink RW. Carbon capture by sorption-enhanced water-gas shift reaction process using hydrotalcite-based material. *Ind Eng Chem Res* 2009;48:4184–4193. [\[CrossRef\]](#)
- [16] dos Santos-Gómez L, Cuesta N, Cameán I, García-Granda S, García AB, Arenillas A. A promising silicon/carbon xerogel composite for high-rate and high-capacity lithium-ion batteries. *Electrochim Acta* 2022;426:140790. [\[CrossRef\]](#)
- [17] Du G, Seng KH, Guo Z, Liu J, Li W, Jia D, et al. Graphene-V<sub>2</sub>O<sub>5</sub>-nH<sub>2</sub>O xerogel composite cathodes for lithium ion batteries. *RSC Adv* 2011;1:690. [\[CrossRef\]](#)
- [18] Guzel Kaya G, Devci H. Synergistic effects of silica aerogels/xerogels on properties of polymer composites: A review. *J Ind Eng Chem* 2020;89:13–27. [\[CrossRef\]](#)
- [19] Owens GJ, Singh RK, Foroutan F, Alqaysi M, Han CM, Mahapatra C, et al. Sol-gel based materials for biomedical applications. *Prog Mater Sci* 2016;77:1–79. [\[CrossRef\]](#)
- [20] Okada K, Kaneda A, Kameshima Y, Yasumori A. Acidic and basic gas adsorption properties in composites of layered double hydroxide/aluminosilicate xerogels. *Mater Res Bull* 2002;37:209–219. [\[CrossRef\]](#)
- [21] Sezgin D, Sari Yilmaz M. Xerogel of fast kinetics and high adsorption capacity for cationic dye removal. *Sigma J Eng Nat Sci* 2024;42:189–197. [\[CrossRef\]](#)
- [22] Hu W, Li M, Chen W, Zhang N, Li B, Wang M, et al. Preparation of hydrophobic silica aerogel with kaolin dried at ambient pressure. *Colloids Surf A Physicochem Eng Asp* 2016;501:83–91. [\[CrossRef\]](#)
- [23] Estella J, Echeverría JC, Laguna M, Garrido JJ. Effects of aging and drying conditions on the structural and textural properties of silica gels. *Micropor Mesopor Mat* 2007;102:274–282. [\[CrossRef\]](#)
- [24] Sari Yilmaz M, Dere Özdemir Ö, Pişkin S. Synthesis and characterization of MCM-41 with different methods and adsorption of Sr<sup>2+</sup> on MCM-41. *Res Chem Intermed* 2015;41:199–211. [\[CrossRef\]](#)

- [25] Sari Yilmaz M, Piskin S. Evaluation of novel synthesis of ordered SBA-15 mesoporous silica from gold mine tailings slurry by experimental design. *J Taiwan Inst Chem Eng* 2015;46:176–182. [\[CrossRef\]](#)
- [26] Mohammadian M, Kashi TSJ, Erfan M, Soorbaghi FP. Synthesis and characterization of silica aerogel as a promising drug carrier system. *J Drug Deliv Sci Technol* 2018;44:205–212. [\[CrossRef\]](#)
- [27] Barahuie F, Hussein MZ, Arulselvan P, Fakurazi S, Zainal Z. Drug delivery system for an anticancer agent, chlorogenate-Zn/Al-layered double hydroxide nanohybrid synthesised using direct co-precipitation and ion exchange methods. *J Solid State Chem* 2014;217:31–41. [\[CrossRef\]](#)
- [28] dos Santos RMM, Gonçalves RGL, Constantino VRL, Santilli CV, Borges PD, Tronto J, et al. Adsorption of acid yellow 42 dye on calcined layered double hydroxide: Effect of time, concentration, pH and temperature. *Appl Clay Sci* 2017;140:132–139. [\[CrossRef\]](#)
- [29] Auxilio AR, Andrews PC, Junk PC, Spiccia L. The adsorption behavior of C.I. Acid Blue 9 onto calcined Mg-Al layered double hydroxides. *Dye Pigment* 2009;81:103–112. [\[CrossRef\]](#)
- [30] Jia Z, Li Z, Ni T, Li S. Adsorption of low-cost absorption materials based on biomass (*Cortaderia selloana* flower spikes) for dye removal: kinetics, isotherms and thermodynamic studies. *J Mol Liq* 2017;229:285–292. [\[CrossRef\]](#)
- [31] Ho YS, McKay G. The kinetics of sorption of basic dyes from aqueous solution by sphagnum moss peat. *Can J Chem Eng* 1998;76:822–827. [\[CrossRef\]](#)
- [32] Serna-Guerrero R, Sayari A. Modeling adsorption of CO<sub>2</sub> on amine-functionalized mesoporous silica. 2: Kinetics and breakthrough curves. *Chem Eng J* 2010;161:182–190. [\[CrossRef\]](#)
- [33] Songolzadeh M, Soleimani M, Takht Ravanchi M. Using modified Avrami kinetic and two component isotherm equation for modeling of CO<sub>2</sub>/N<sub>2</sub> adsorption over a 13X zeolite bed. *J Nat Gas Sci Eng* 2015;27:831–841. [\[CrossRef\]](#)
- [34] Kaya GG, Deveci H. CO<sub>2</sub> capture using polyethyleneimine functionalized silica xerogels. *Konya Müh Bil Derg* 2021;9:1109–1118. [\[CrossRef\]](#)
- [35] Santos LMD, Bernard FL, Pinto IS, Scholer H, Dias GG, Prado M, Einloft S. Polyurethane/ionic silica xerogel composites for CO<sub>2</sub> capture. *Mater Res* 2019;22:e20190022. [\[CrossRef\]](#)
- [36] Kou X, Guo H, Ayele EG, Li S, Zhao Y, Wang S, Ma X. Adsorption of CO<sub>2</sub> on MgAl-CO<sub>3</sub> LDHs-derived sorbents with 3D nanoflower-like structure. *Energy Fuel* 2018;32:5313–5320. [\[CrossRef\]](#)
- [37] Gunjekar JL, Kim IY, Hwang SJ. Efficient hybrid-type CO<sub>2</sub> Adsorbents of reassembled layered double hydroxide 2D nanosheets with polyoxometalate 0D nanoclusters. *Eur J Inorg Chem* 2015;7:1198–1202. [\[CrossRef\]](#)
- [38] Iruretagoyena D, Shaffer MS, Chadwick D. Layered double oxides supported on graphene oxide for CO<sub>2</sub> adsorption: Effect of support and residual sodium. *Ind Eng Chem Res* 2015;54:6781–6792. [\[CrossRef\]](#)